PAPER

Check for updates

Innovative hafnium composite: efficient fabrication and advanced biomedical potential in dentistry and oral health

Fadhil Faez Sead,[akl] Ahmed Aldulaimi,[b] Farag M. A. Altalbawy,[c] Shakir Mahmood Saeed,[d] Samah Naem,[e] Issa Mohammed Kadhim,[f] Waam mohammed taher,[g] Khursheed Muzammil, [ID][h] Aseel Smerat[im] and Mohammad Al Hesani [ID] *[j]

The development of multifunctional dental coatings capable of preventing biofilm formation and promoting oral tissue health is a growing focus in modern restorative dentistry. In this study, a novel hafnium-based metal–organic framework was synthesized *via* a rapid microwave-assisted method using 4-aminopyridine-2,6-dicarboxylic acid as the organic linker. The synthesized MOF was abbreviated as Hf/APDC-MOF, derived from the names of its components (hafnium 4-aminopyridine-2,6-dicarboxylic acid metal–organic framework). The synthesized MOF was designed for potential use as a bioactive dental surface coating with broad-spectrum therapeutic functions. The material demonstrated strong antibacterial activity against key oral pathogens, including *Streptococcus mutans* and *Porphyromonas gingivalis*, with minimum inhibitory concentration (MIC) values of 1 μg mL^{-1}. *In vitro* cytotoxicity testing using the MTT assay revealed selective anticancer effects against SCC154 (CRL-3241) gingival carcinoma cells, with an IC$_{50}$ value of 78 μg mL^{-1}. Additionally, the MOF exhibited high antioxidant capacity (79% DPPH radical scavenging at 100 μg mL^{-1}) and effective anti-inflammatory activity by reducing nitric oxide production by 74% in LPS-stimulated RAW 264.7 macrophages. These results suggest that Hf/APDC-MOF is a promising candidate for multifunctional dental coatings, combining antimicrobial protection with antioxidant, anti-inflammatory, and anticancer effects, thereby offering a novel therapeutic platform for oral health management. The synthesized MOF was designed and evaluated *in vitro* as a multifunctional bioactive material with potential relevance to dental surface coatings, combining antimicrobial, antioxidant, anti-inflammatory, and anticancer properties.

[a]Department of Dentistry, College of Dentistry, The Islamic University, Najaf, Iraq
[b]Department of Pharmacy, Al-Zahrawi University, Karbala, Iraq
[c]Department of Chemistry, University College of Duba, University of Tabuk, Tabuk, Saudi Arabia
[d]College of Pharmacy, Alnoor University, Nineveh, Iraq
[e]Department of Dentistry, Al-Manara College for Medical Sciences, Maysan, Iraq
[f]Department of Medical Laboratories Technology, Al-Nisour University College, Nisour Seq. Karkh, Baghdad, Iraq
[g]College of Nursing, National University of Science and Technology, Dhi Qar, Iraq
[h]Department of Public Health, College of Applied Medical Sciences, Khamis Mushait Campus, King Khalid University, Abha, 62561, Saudi Arabia
[i]Faculty of Educational Sciences, Al-Ahliyya Amman University, Amman 19328, Jordan
[j]Department of Pharmacy, Faculty of Medicine and Health Sciences, Hadhramout University, Mukalla, Yemen. E-mail: alhesanimohammad@gmail.com
[k]Department of Medical Analysis, Medical Laboratory Technique College, The Islamic University of Al Diwaniyah, Al Diwaniyah, Iraq
[l]Department of Medical Analysis, Medical Laboratory Technique College, The Islamic University of Babylon, Babylon, Iraq
[m]Department of Biosciences, Saveetha School of Engineering, Saveetha Institute of Medical and Technical Sciences, Chennai, 602105, India

Introduction

Maintaining the integrity of dental restorations and preventing microbial colonization at the tooth–material interface remain significant challenges in restorative dentistry.[1] Biofilm formation on dental surfaces can lead to secondary caries, peri-implantitis, and implant failure, negatively affecting patient outcomes.[2] Conventional dental materials often lack intrinsic bioactivity, limiting their ability to combat oral pathogens, reduce oxidative stress, or modulate inflammatory responses.[3] Therefore, developing multifunctional dental coatings with combined antibacterial, antioxidant, anti-inflammatory, and anticancer properties is essential to improve oral health and extend the longevity of dental prosthetics.

Conventional dental coating materials, such as titanium oxide and hydroxyapatite-based composites, provide mechanical protection but often lack integrated biological functions such as antimicrobial or anti-inflammatory activity. In contrast, metal–organic frameworks offer a platform for designing multifunctional materials that can simultaneously address

microbial colonization, oxidative stress, and inflammation, potentially complementing existing dental coating technologies.

Metal–organic frameworks (MOFs) have recently emerged as a versatile class of porous materials characterized by high surface area,[4] tunable pore size,[5] and chemical versatility,[6] making them promising candidates for biomedical applications, such as, drug delivery,[7] imaging,[8] and tissue engineering.[9] Among MOFs, hafnium-based frameworks (Hf-MOFs) have attracted attention due to their excellent chemical and thermal stability,[10] low toxicity,[11] and favorable biocompatibility.[11] Hafnium ions (Hf[4+]) contribute to the formation of robust coordination networks and have been associated with moderate intrinsic antibacterial activity, positioning Hf-MOFs as attractive materials for biofunctional coatings.[11,12]

The choice of organic linker plays a critical role in determining the biological activity of MOFs.[13] 4-Aminopyridine-2,6-dicarboxylic acid, a pyridine-based ligand containing nitrogen and oxygen donor atoms, offers multiple coordination sites and potential biological functions.[14] Aminopyridine derivatives have demonstrated diverse biological properties, including antibacterial,[15] antioxidant,[16] anti-inflammatory,[17] and anticancer activities.[18] The amino group is known to contribute to free radical scavenging and modulate immune responses, while the pyridine ring enhances molecular interactions with biological targets.[19,20] Such multifunctional bioactivity suggests that MOFs constructed with 4-aminopyridine-based ligands may provide enhanced therapeutic effects.[21]

Microwave-assisted synthesis is an efficient and environmentally friendly technique for producing MOFs, offering rapid reaction rates, improved crystallinity, and uniform particle size distribution compared to conventional methods.[22] Despite these advantages, the microwave synthesis of Hf-MOFs incorporating bioactive aminopyridine ligands for dental coating applications has been scarcely explored.

To date, no studies have reported the development of a hafnium-based metal–organic framework constructed with 4-aminopyridine-2,6-dicarboxylic acid (Hf/APDC-MOF) *via* microwave-assisted synthesis for dental biomedical applications. This study introduces a novel Hf/APDC-MOF with potential use as a multifunctional dental coating, combining structural stability with biologically relevant functionality. The simultaneous integration of antibacterial, anticancer, antioxidant, and anti-inflammatory properties into a single MOF system, evaluated specifically in the context of oral pathogens and gingival carcinoma cells, offers a unique approach not previously explored in the field of dental materials. This work bridges the gap between advanced MOF chemistry and the emerging demand for bioactive dental surface technologies.

Results

Structural and characterization

The synthesized Hf/APDC-MOF or hafnium-based metal–organic framework, formed by coordination of Hf[4+] with 4-aminopyridine-2,6-dicarboxylic acid.
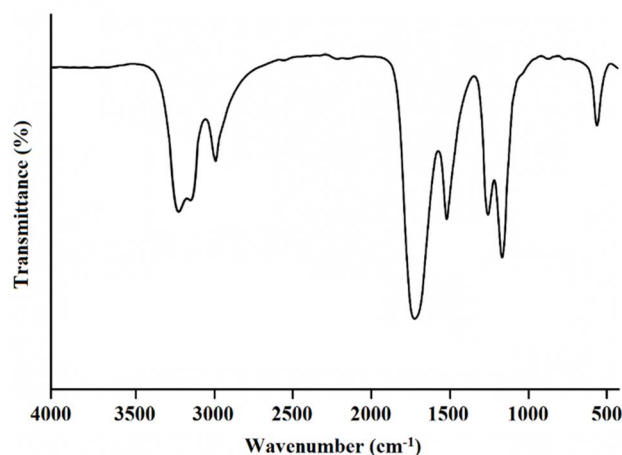

Fig. 1 FT-IR spectrum of the Hf/APDC-MOF.

Fourier transform infrared spectroscopy (FT-IR). The FT-IR spectrum of the synthesized Hf/APDC-MOF (Fig. 1) reveals a range of characteristic absorption bands confirming the successful coordination of the ligand through its carboxylate groups to the Hf[4+] center. The strong absorption band around 3200–3300 cm^{-1} corresponds to N–H stretching of the free amine group (–NH$_2$), indicating that the amine moiety did not participate in metal coordination. Additional notable vibrations include:

1100 cm^{-1} for C–O of carboxylat,
1350 cm^{-1} for aromatic C=C,
1500 cm^{-1} for C=N in the pyridine ring,
1700 cm^{-1} for C=O of carboxylat,
2990 cm^{-1} for aromatic C–H,
560 cm^{-1} corresponding to Hf–O.

X-ray diffraction (XRD). The XRD pattern revealed sharp diffraction peaks (Fig. 2), confirming the crystalline nature of the synthesized MOF. The XRD pattern of the synthesized Hf/APDC-MOF shows sharp and well-defined peaks at 2θ values of 10.5°, 14.4°, 19.2°, 25.7°, 29.8°, and 34.1°, indicating a high degree of crystallinity. The absence of extra peaks suggests
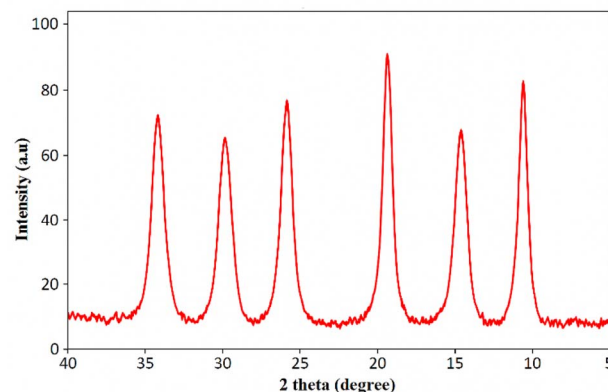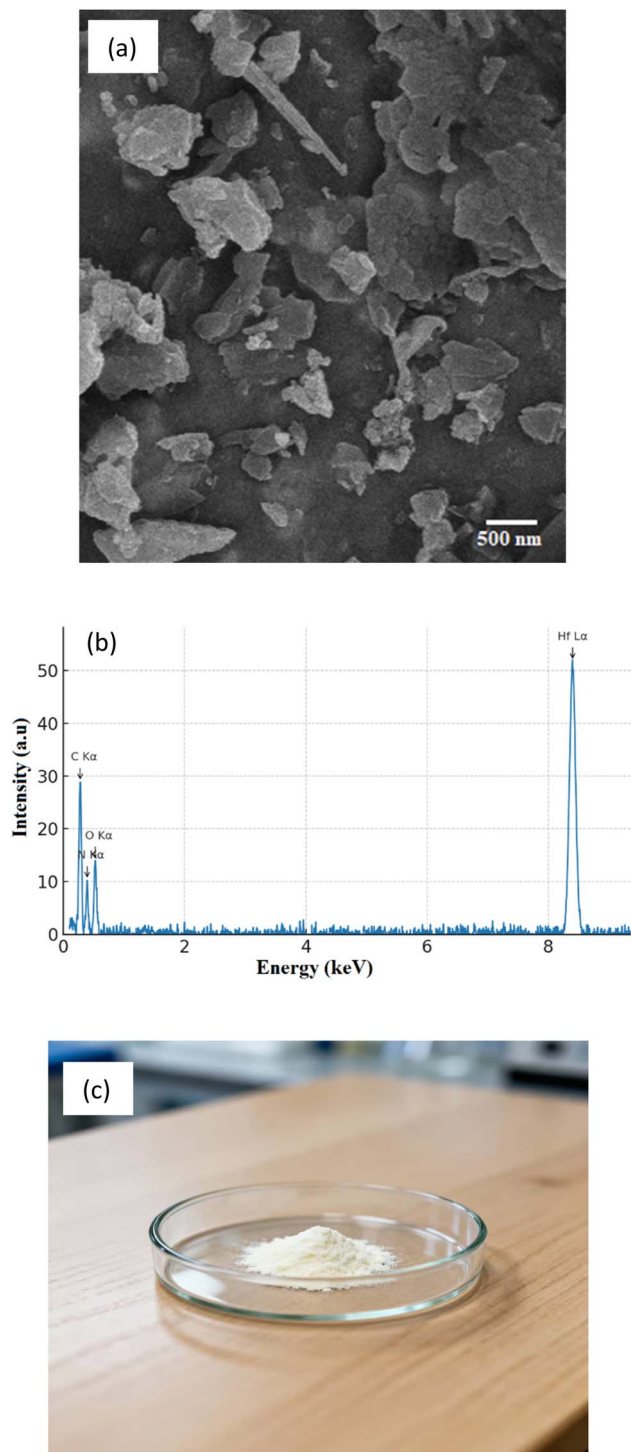

Fig. 2 XRD of the Hf/APDC-MOF.

Fig. 3 SEM (a), EDAX (b) and physical photo (c) of the Hf/APDC-MOF.

phase purity. The pattern matches closely with previously reported Hf-based MOFs.[23]

Using XPS (Fig. 4), the binding energies were observed to be 63.6 eV, 66.2 eV, 285.1 eV, and 529.4 eV and 530.7 eV.

Scanning electron microscopy (SEM) and EDAX. SEM analysis showed that the particles possessed uniform nanocrystalline morphology with sizes ranging from approximately 76 nm (Fig. 3a). The relatively small particle size enhances surface contact with biological environments.[24] EDAX elemental mapping confirmed the homogeneous distribution of Hf, C, N, and O elements across the surface, aligning well with the proposed MOF composition (Fig. 3b). The physical photo of the final product is shown in Fig. 3c.

Elemental analysis. In elemental analysis (CHNO) carbone 24.1%, hydrogen 1.7%, nitrogen 7.5%, and oxygen 13.4% obtained.

BET surface area and porosity. The N_2 adsorption–desorption isotherm of the Hf/APDC-MOF (Fig. 4) exhibits a type IV profile with a pronounced hysteresis loop in the mid-relative pressure range, consistent with a mesoporous structure.[24,25] BET analysis yields a specific surface area of 560 m^2 g^{-1} (Fig. 4). The total pore volume at $P/P_0 \approx 0.99$ is 0.42 cm^3 g^{-1} and the average pore diameter (BJH desorption) is 3.2 nm. The observed capillary condensation in the $P/P_0 \approx 0.4$–0.7 region and the hysteresis loop are consistent with mesopores in the 2–5 nm range; the hysteresis shape relatively uniform mesopores (H1-type).[26] These textural parameters indicate a high capacity for uptake of small organic molecules and radicals (e.g., DPPH) and good potential for loading small-molecule therapeutics; however, the pore size is far too small to physically accommodate whole bacterial or mammalian cells.[27,28]

Thermogravimetric analysis (TGA). Room temperature to 150 °C: a small weight loss of 3% is expected, attributed to desorption of weakly bound solvent or surface-adsorbed moisture.

150–300 °C: an additional 10% mass loss is predicted, which likely reflects the partial decomposition or release of labile ligand fragments (e.g., carboxylate cleavage and loss of small volatile nitrogen-containing species).

300–550 °C: the principal decomposition event is anticipated in this interval with a further 30% mass loss, corresponding to degradation of the aromatic pyridine units and carbonaceous components of the organic framework (Fig. 5).

Proposed structure of Hf/APDC-MOF. Based on the coordination chemistry of 4-aminopyridine-2,6-dicarboxylic acid, it is proposed that the carboxylate groups are solely responsible for coordination with the Hf^{4+} centers. Each Hf^{4+} ion is likely
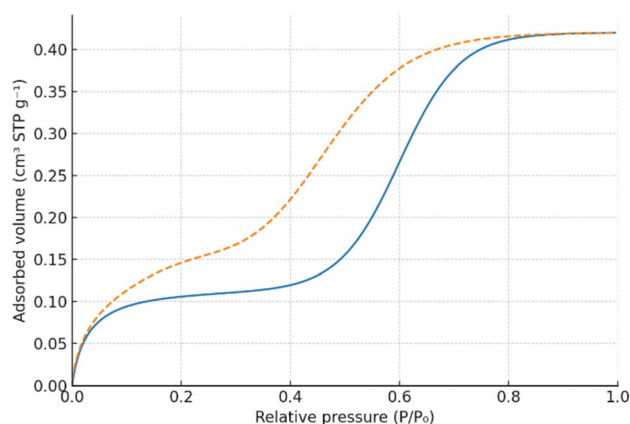

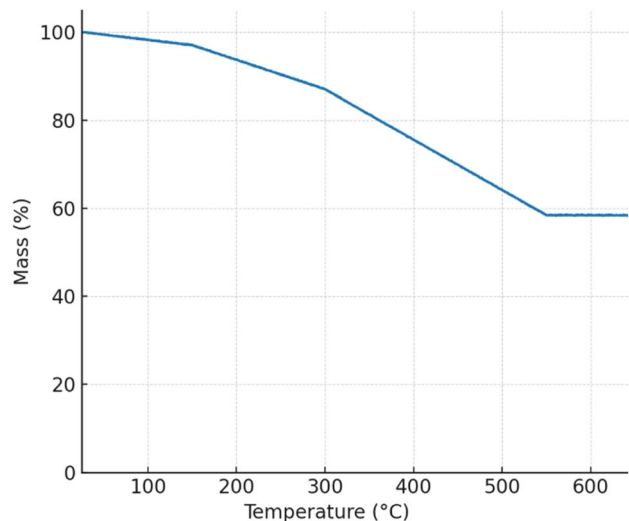Fig. 4 N_2 adsorption–desorption of the Hf/APDC-MOF.
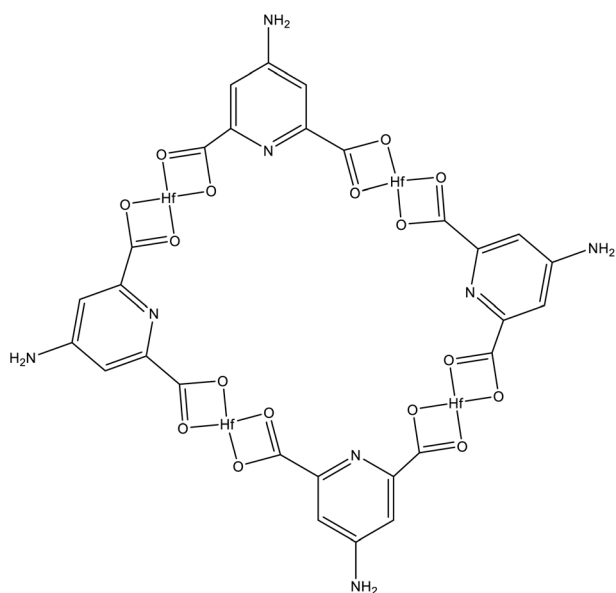
Fig. 5   TGA curve of the Hf/APDC–MOF.

Fig. 6   Structure of the Hf/APDC–MOF.

Fig. 7   Antimicrobial activity of the Hf/APDC-MOF (mean ± SD, $n = 3$; $p < 0.05$ compared to control).
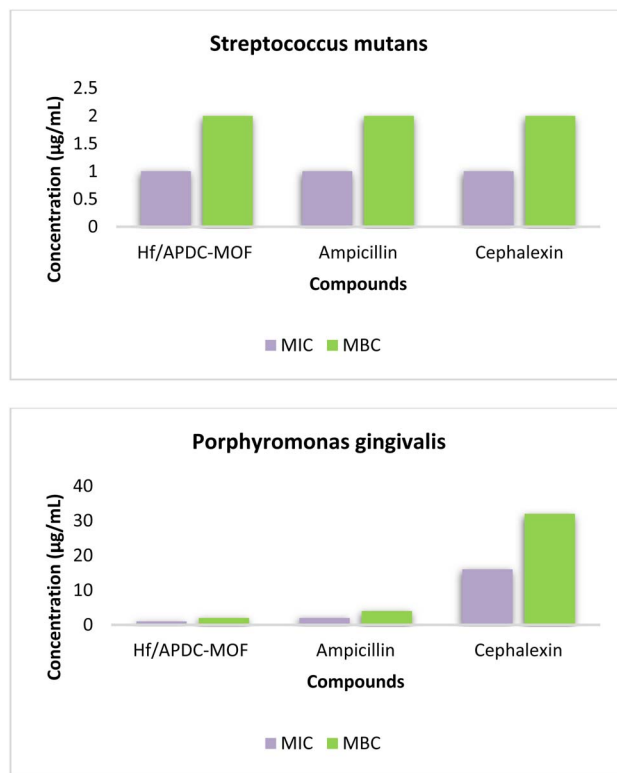
coordinated octahedrally or in a higher coordination geometry with multiple carboxylate ligands, forming a three-dimensional porous framework. The –NH₂ group remains uncoordinated and is exposed on the internal pore surfaces or external surface of the Hf/APDC-MOF particles. This structural feature may enhance the material's ability to scavenge radicals and interact with biological targets *via* hydrogen bonding or electron donation (Fig. 6).

Biological activity results

Antibacterial activity results. The MIC and MBC of the Hf/APDC-MOF were evaluated against pathogenic oral bacterial strains including *Streptococcus mutans* and *Porphyromonas gingivalis* (Fig. 7).

The results are summarized as follows:

MIC against *S. mutans* and *P. gingivalis*: 1 µg mL⁻¹.

MBC against *S. mutans* and *P. gingivalis*: 2 µg mL⁻¹.

In addition, the antibacterial performance of the synthesized Hf/APDC-MOF was compared with two commercial antibiotics (ampicillin and cephalexin). Notably, the Hf/APDC-MOF exhibited stronger antibacterial activity than ampicillin and cephalexin against both tested strains.

The results are summarized as follows:

MIC of ampicillin and cephalexin against *S. mutans*: 1 µg mL⁻¹.

MBC of ampicillin and cephalexin against *S. mutans*: 2 µg mL⁻¹.

MIC of ampicillin and cephalexin against *P. gingivalis*: 2 µg mL⁻¹ and 16 µg mL⁻¹.

MBC of ampicillin and cephalexin against *P. gingivalis*: 4 µg mL⁻¹ and 32 µg mL⁻¹.

Anticancer activity results. The anticancer potential of the Hf/APDC-MOF was assessed on the SCC154 (CRL-3241) human gingival squamous carcinoma cell line using the MTT assay (Fig. 8). Cell viability decreased in a concentration and time-dependent manner.

The results are summarized as follows:

IC₅₀ value (24 h): 119 µg mL⁻¹.

IC₅₀ value (48 h): 78 µg mL⁻¹.

Viability at 200 µg mL⁻¹ (24 h): 30%.

Viability at 200 µg mL⁻¹ (48 h): 17%.

Fig. 8 Anticancer activity of the Hf/APDC-MOF (mean ± SD, n = 3; p < 0.05 compared to control).

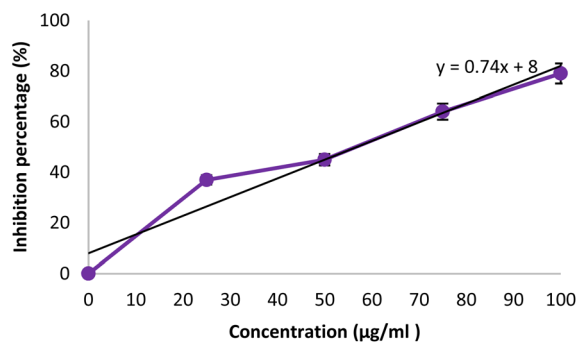Fig. 10 Anti-inflammatory activity of the Hf/APDC-MOF (mean ± SD, n = 3; p < 0.05 compared to control).

Fig. 9 Antioxidant activity of the Hf/APDC-MOF (mean ± SD, n = 3; p < 0.05 compared to control).

NO concentration at 100 μg mL^{-1}: 26%.

NO inhibition at 25 μg mL^{-1}: 23%.

NO inhibition at 100 μg/mL74%.

IC_{50} for NO inhibition 66 μg mL^{-1}.

Discussion

Hf/APDC-MOF synthesis discussion

The microwave-assisted method offered significant advantages including shorter reaction time, uniform heating, and improved crystallinity.[29] The optimized synthesis conditions led to the formation of a highly porous, nanostructured Hf/APDC-MOF with uniform morphology and enhanced stability. These structural and physicochemical features are expected to contribute to its superior biological properties,[4] which are discussed in detail in the following sections.

Biological activity discussion

Antibacterial activity discussion. The synthesized Hf/APDC-MOF demonstrated significant antibacterial activity against *Streptococcus mutans* and *Porphyromonas gingivalis*. MIC values was 1 μg mL^{-1}. The Hf/APDC-MOF had a strong inhibitory effect than ampicillin and cephalexin against *Porphyromonas gingivalis*. The antibacterial mechanism is likely driven by a combination of nanoscale size (increasing interaction with bacterial membranes),[30] high surface area (enhancing local concentration of active species),[31] intrinsic antimicrobial properties of

Antioxidant activity results. DPPH radical scavenging activity was performed to evaluate the antioxidant capability of the Hf/APDC-MOF (Fig. 9).

The results are summarized as follows:

Radical inhibition at 25 μg mL^{-1}: 37%.

Radical inhibition at 100 μg mL^{-1}: 79%.

IC_{50} value: 58 μg mL^{-1}.

Anti-inflammatory activity results. Nitric oxide inhibition in LPS-stimulated macrophages was used to determine anti-inflammatory activity of Hf/APDC-MOF (Fig. 10).

The results are summarized as follows:

NO concentration at 25 μg mL^{-1}: 87%.

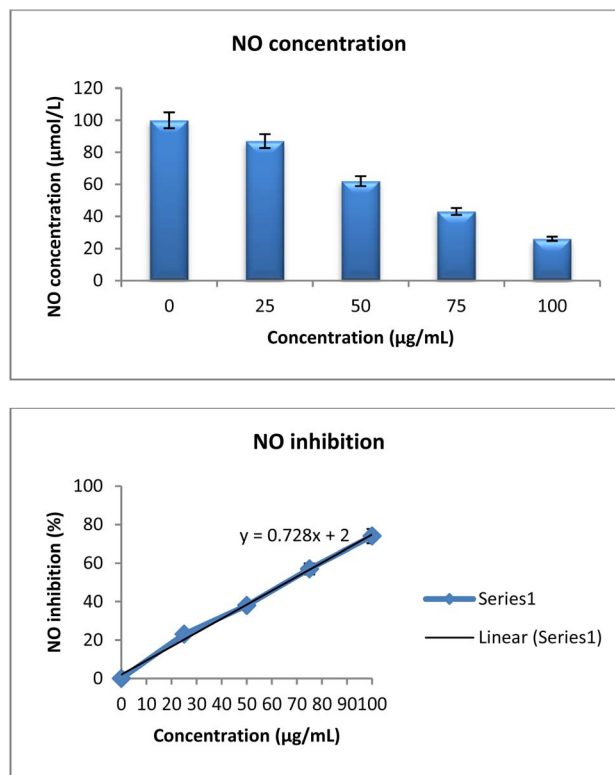Hf^{4+},[32] and active –NH_2 functionalities capable of interacting with bacterial membranes which may disrupt bacterial enzymatic pathways or induce oxidative stress.[33,34]

Anticancer activity discussion. The Hf/APDC-MOF showed strong cytotoxicity against SCC154 gingival carcinoma cells, with a marked dose-dependent reduction in cell viability. This may stem from the material's ability to generate localized oxidative stress, disrupt membrane potential, or induce apoptosis through interaction with intracellular proteins.[35] The high surface area facilitates contact and cellular uptake, while the Hf^{4+} centers may contribute to ROS generation or DNA binding.[36]

Antioxidant activity discussion. Interestingly, the Hf/APDC-MOF exhibited notable DPPH radical scavenging activity. This is attributed primarily to the presence of free –NH_2 groups on the ligand, which can donate hydrogen atoms to stabilize free radicals.[37,38] Additionally, the high surface area and porous nature of the MOF allows better diffusion and adsorption of DPPH molecules, enhancing the effectiveness of radical neutralization.[39] The proposed mechanism for the absorption of DPPH free radical by Hf/APDC-MOF is shown in Fig. 11.

In explaining the proposed mechanism, it can be said that, as previously mentioned, one of the important factors is the absorption of DPPH inside the pores of the Hf/APDC-MOF. Also the absorption of free radicals by the Hf/APDC-MOF nitrogen's and the multiplicity of resonance structures can be mentioned as other important factors for the high antioxidant properties of the Hf/APDC-MOF.[40,41]

Anti-inflammatory activity discussion. The Hf/APDC-MOF effectively reduced nitric oxide (NO) production in LPS-stimulated macrophages, indicating its anti-inflammatory potential. This effect may be related to its capacity to modulate oxidative stress or interfere with nitric oxide synthase activity.[42] The combined contributions of Hf^{4+} ions and the organic framework appear to downregulate the inflammatory signaling cascade.[32]

Compared with conventional dental coating materials (*e.g.*, TiO_2, hydroxyapatite, and polymer-based composites), the Hf/APDC-MOF exhibits an expanded spectrum of biological activity, particularly due to the presence of uncoordinated –NH_2 groups and Hf^{4+} centers contributing to synergistic antibacterial and antioxidant functions. Although mechanical and

adhesion performance were not assessed in this study, the observed *in vitro* bioactivity suggests the material could serve as a functional additive or coating component in future dental restorative systems.

Experimental

Materials

Hafnium(IV) chloride ($HfCl_4$): purchased from Sigma-Aldrich (≥99.9% purity). Used as the hafnium metal source for MOF synthesis. 4-Aminopyridine-2,6-dicarboxylic acid (APDC): purchased from TCI Chemicals (Tokyo Chemical Industry) or Sigma-Aldrich, analytical grade. This ligand acts as the organic linker in the framework.

Cell lines: human gingival squamous cell carcinoma (SCC154, CRL-3241), and RAW 264.7 macrophage cells (TIB-71) were obtained from the ATCC (American Type Culture Collection, USA). Bacterial strains: oral bacteria strains (*Streptococcus mutans*/ATCC 25175 and *Porphyromonas gingivalis*/ATCC 33277) were procured from ATCC.

Other chemicals and reagents were purchased from commercial suppliers with analytical grade purity.

Equipment

Synthesis equipment. In this study, the microwave reactor (CEM Discover SP, NC, USA), used for rapid and controlled microwave-assisted synthesis of the Hf/APDC-MOF.

Characterization equipment. The following equipment was used to characterization of the final product:

FEG Quanta 250 SEM (Thermo Fisher Scientific, USA): for morphological and surface structure analysis (Scanning Electron Microscope/SEM). ASAP 2020 (Micromeritics, USA): for specific surface area and porosity measurement (Brunauer–Emmett–Teller/BET). Nicolet iS50 (Thermo Fisher Scientific, USA): for identification of functional groups and coordination bonds (Fourier Transform Infrared Spectrometer/FT-IR). Oxford Instruments X-Max 80 detector coupled with SEM: for elemental composition analysis (Energy Dispersive X-ray Analysis/EDAX). TA Instruments Q50 (TA Instruments, USA): for thermal stability assessment under nitrogen atmosphere (Thermogravimetric Analyzer/TGA). PA Nalytical Empyrean (Malvern Panalytical, Netherlands) with Cu-Kα radiation: for phase and crystallinity determination (X-ray Diffractometer/XRD). Vario EL III (Elementar Analysensysteme GmbH, Germany): for carbon, hydrogen, and nitrogen content analysis (Elemental Analyzer).

Biological testing equipment. The following equipment was used to biological testing:

BioTek Synergy H1 (BioTek Instruments, USA) microplate reader used for MTT and Griess assays with absorbance measurements at relevant wavelengths.

LAMBDA 365 (PerkinElmer, USA) UV-visible spectrophotometer for prepare bacterial suspension concentration and DPPH assays absorbance.
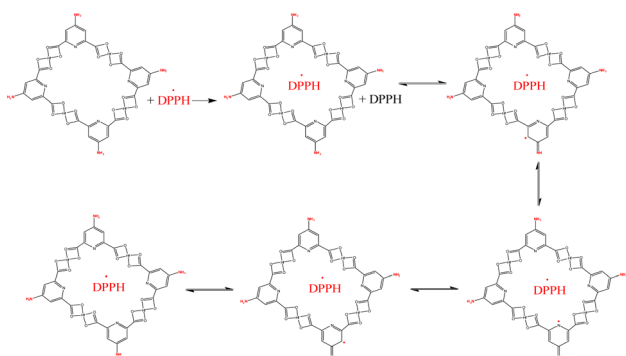

Fig. 11 Antioxidant activity of the Hf/APDC-MOF.

Methods

Synthesis of Hf/APDC-MOF. The Hf/APDC-MOF was synthesized using a microwave-assisted. A stoichiometric mixture of HfCl$_4$ (0.2 mmol, 64 mg) and 4-aminopyridine-2,6-dicarboxylic acid (0.2 mmol, 38 mg) was dissolved in a mixture of DMF (10 mL) and distilled water (2 mL). The solution was transferred into a microwave reactor and irradiated at 100 °C for 30 minutes under a power of 320 W. After cooling, the Hf/APDC-MOF was collected by centrifugation and washed three times with ethanol : water (1 : 1), and dried under vacuum at 100 °C overnight.[43,44]

Antibacterial activity. The antibacterial activity of Hf/APDC-MOF was evaluated against oral bacteria strains (*Porphyromonas gingivalis* and *Streptococcus mutans*). The MIC (minimum inhibitory concentration) and MBC (minimum bactericidal concentration) were determined by broth microdilution method according to CLSI guidelines. Briefly, bacterial suspensions were prepared in Mueller–Hinton broth at 1×10^6 CFU mL^{-1}. Serial two-fold dilutions of Hf-MOF (1 to 512 µg mL^{-1}) were prepared in 96-well microplates. To each well added bacterial suspension and incubated at 37 °C for 24 hours. After incubation, bacterial growth was assessed visually by observing the turbidity of each well. The MIC was defined as the lowest concentration at which no visible bacterial growth (clear well) was observed. For MBC determination, aliquots from wells showing no visible growth were plated on Mueller–Hinton agar plates and incubated for an additional 24 hours. The MBC was recorded as the lowest concentration of Hf-MOF resulting in no bacterial colony formation.[45–47]

Anticancer activity. The cytotoxicity (MTT assay) of the Hf/APDC-MOF was assessed against human gingival squamous cell carcinoma SCC154, CRL-3241. Cells were cultured in Dulbecco's Modified Eagle Medium (DMEM) supplemented with 10% fetal bovine serum and incubated at 37 °C with 5% CO$_2$. After reaching 70–80% confluence, cells were seeded into 96-well plates at a density of 1×10^4 cells/well and allowed to adhere overnight. Cells were treated with various concentrations of Hf/APDC-MOF (ranging from 5 to 200 µg mL^{-1}) for 24 hours and 48 hours. Subsequently, 20 µL of MTT solution in PBS with concentrations of 5 mg mL^{-1} was added to each well and incubated for 4 h. Then the formed formazan dissolved in 150 µL dimethyl sulfoxide (DMSO), and absorbance was measured at 570 nm. Cell viability was calculated relative to untreated control cells.[45,48,49]

Antioxidant activity. The free radical scavenging ability of the Hf/APDC-MOF was evaluated using the DPPH assay (2,2-diphenyl-1-picrylhydrazyl). A 0.1 mM DPPH solution was prepared in methanol. 1 mmL of various concentrations of Hf-MOF (25–100 µg mL^{-1}) were mixed with 4 mL of DPPH solution in the dark at room temperature for 30 minutes. Absorbance was measured at 517 nm. The percentage of DPPH radical scavenging activity was calculated relative to a blank control without the sample.[50–52]

Anti-inflammatory activity. Nitric oxide (NO) production in lipopolysaccharide (LPS)-stimulated RAW 264.7 macrophage cells (Griess assay) used to anti-inflammatory potential of Hf/APDC-MOF. The RAW 264.7 cells were cultured in DMEM with 10% fetal bovine serum and seeded in 96-well plates at a density of 1×10^5 cells/well. After 24 hours, cells were pre-treated with Hf-MOF (25–100 µg mL^{-1}) for 1 hour, followed by stimulation with LPS (1 µg mL^{-1}) for 24 hours. The culture supernatant (100 µL) was mixed with an equal volume of Griess reagent and incubated at room temperature for 10 minutes. The absorbance was recorded at 540 nm. Nitrite concentration was calculated from a sodium nitrite standard curve to quantify NO production.[53,54]

Statistical analysis. All experiments were performed in triplicate ($n = 3$), and the data are expressed as mean ± standard deviation (SD). Statistical differences between control and treated groups were analyzed using one-way ANOVA followed by Tukey's *post hoc* test (GraphPad Prism 9.0). A *p*-value less than 0.05 was considered statistically significant.

Conclusions

In this study, a novel hafnium-based metal–organic framework (Hf/APDC-MOF) was successfully synthesized using 4-aminopyridine-2,6-dicarboxylic acid as a multifunctional organic linker under microwave-assisted conditions. Comprehensive physicochemical characterizations including FT-IR, XRD, SEM, BET, TGA, EDAX, and elemental analysis confirmed the formation of a crystalline, thermally stable, and mesoporous nanostructure with abundant surface functionalities. The Hf/APDC-MOF exhibited promising multifunctional biological properties, including potent antibacterial activity against oral pathogens, selective cytotoxicity against gingival carcinoma cells, significant antioxidant performance in the DPPH assay, and strong anti-inflammatory activity through nitric oxide inhibition. These effects are attributed to the nanostructured porous architecture, high surface area, and the presence of biologically active components such as Hf^{4+} ions and uncoordinated –NH$_2$ groups on the ligand backbone. Given its broad-spectrum bioactivity and physicochemical stability, the synthesized Hf/APDC-MOF presents itself as a potential candidate for application in biofunctional dental coatings. Its antimicrobial, anticancer, antioxidant, and anti-inflammatory activities suggest its utility in oral healthcare devices aiming at preventing secondary infections, enhancing tissue regeneration, and supporting local cancer therapy. Further *in vivo* studies and surface modification strategies could pave the way for its translation into clinical-grade dental biomaterials. Within the limits of the *in vitro* assessments conducted in this study, the Hf/APDC-MOF exhibits promising multifunctional bioactivity that could inform the design of future biofunctional dental coatings. Further *in vivo* and long-term studies are essential to establish its safety, stability, and translational potential for oral healthcare applications. Although the present study focused on *in vitro* antibacterial, anticancer, antioxidant, and anti-inflammatory performance, comprehensive biocompatibility assessment, including cytotoxicity toward normal oral cells and hemolysis testing, will be conducted in future work to confirm the material's safety for clinical translation.

Limitations

Despite the promising biological performance and structural features of the synthesized Hf/APDC-MOF, several limitations should be acknowledged.

Lack of *in vivo* validation

All biological evaluations in this study were performed *in vitro*. While these results provide a strong foundation, the actual performance of the material in complex biological environments, such as in the oral cavity or cancerous tissues, remains untested.

Long-term biocompatibility and degradation

The long-term biocompatibility, degradation profile, and potential toxicity of the Hf/APDC-MOF have not been assessed. These factors are critical for clinical applications, especially for dental coatings or implantable devices.

Release kinetics of bioactive ions

Although biological activities were demonstrated, the release behavior of Hf^{4+} ions or any possible degradation products was not investigated, which limits understanding of the material's mechanism of action and safety profile.

Limited pathogen and cell line scope

The antibacterial and anticancer evaluations were limited to selected bacterial strains and a single oral cancer cell line (SCC154). Broader screening across multiple pathogens and cancer types would provide a more comprehensive view of the material's therapeutic potential.

Scalability and reproducibility

Although microwave-assisted synthesis is efficient, scalability to industrial or clinical-scale production has not yet been optimized or evaluated for reproducibility under large-batch conditions.

Author contributions

FFS: writing – original draft, formal analysis; AA: writing – original draft, methodology; FMAA: writing – review and editing, formal analysis; SMS: writing – original draft, conceptualization; SN: writing – review and editing, data curation; IMK: writing – original draft, formal analysis; WMT: writing – review and editing, resources; KM: writing – original draft, writing – review and editing, validation. AS: writing – review and editing, investigation; MA: writing – original draft, writing – review and editing, visualization. All authors approved the final version of the manuscript.

Conflicts of interest

There are no conflicts to declare.

Data availability

The data supporting this article have been included in article.

Acknowledgements

References

1 C. S. Pfeifer, F. S. Lucena and F. M. Tsuzuki, *J. Funct. Biomater.*, 2025, **16**, 42.

2 Z. Cui, P. Wang and W. Gao, *Front. Cell. Infect. Microbiol.*, 2025, **15**, 1517154.

3 M. A. Anwar, G. A. Sayed, D. M. Hal, M. S. A. E. Hafeez, A.-A. S. Shatat, A. Salman, N. M. Eisa, A. Ramadan, R. A. El-Shiekh and S. Hatem, *Inflammopharmacology*, 2025, **33**, 1085–1160.

4 H. R. Abid, M. R. Azhar, S. Iglauer, Z. H. Rada, A. Al-Yaseri and A. Keshavarz, *Heliyon*, 2024, **10**(1), e23840.

5 K. Liang, W. Guo, L. Li, H. Cai, H. Zhang, J. Li, F. Xu, J. Yan, D. Lv and H. Xi, *Nano Mater. Sci.*, 2024, **6**, 467–474.

6 C. Carbonell, M. Linares-Moreau, S. M. Borisov and P. Falcaro, *Adv. Mater.*, 2024, **36**, 2408770.

7 B. Saboorizadeh, R. Zare-Dorabei, M. Safavi and V. Safarifard, *Langmuir*, 2024, **40**, 22477–22503.

8 I. Abánades Lázaro, X. Chen, M. Ding, A. Eskandari, D. Fairen-Jimenez, M. Giménez-Marqués, R. Gref, W. Lin, T. Luo and R. S. Forgan, *Nat. Rev. Methods Primers*, 2024, **4**, 42.

9 X. Yao, X. Chen, Y. Sun, P. Yang, X. Gu and X. Dai, *Regener. Biomater.*, 2024, **11**, rbae009.

10 R.-L. Liu, H.-M. Ren, S. Zhao, D. Lin, K. Cheng, G. Li and D.-Y. Wang, *Inorg. Chem.*, 2025, **64**, 1183–1192.

11 S. Rojas-Buzo, C. Pontremoli, S. De Toni, K. Bondar, S. Galliano, H. Paja, B. Civalleri, A. Fiorio Pla, C. Barolo and F. Bonino, *ACS Appl. Mater. Interfaces*, 2024, **17**, 524–536.

12 S. Ding, L. Chen, J. Liao, Q. Huo, Q. Wang, G. Tian and W. Yin, *Small*, 2023, **19**, 2300341.

13 M. Ahmadi, S. M. Ayyoubzadeh, F. Ghorbani-Bidkorbeh, S. Shahhosseini, S. Dadashzadeh, E. Asadian, M. Mosayebnia and S. Siavashy, *Heliyon*, 2021, **7**(4), e06914.

14 K. Heise, E. Kontturi, Y. Allahverdiyeva, T. Tammelin, M. B. Linder, Nonappa and O. Ikkala, *Adv. Mater.*, 2021, **33**, 2004349.

15 F. M. Ahamed, A. M. Ali, V. Velusamy and M. Manikandan, *Mater. Today: Proc.*, 2021, **47**, 2053–2061.

16 Y. Hu, J. Zhang, C. Yu, Q. Li, F. Dong, G. Wang and Z. Guo, *Int. J. Biol. Macromol.*, 2014, **70**, 44–49.

17 T. Dimova, P. Rashev, S. Manchev, L. Vezenkov and *Proceedings of the Bulgarian Academy of Sciences*, 2024, vol. 77(11), pp. 1611–1621.

18 S. Mansour, G. Sayed, M. Marzouk and S. Shaban, *Synth. Commun.*, 2021, **51**, 1160–1170.

19 R. Gattu, S. S. Ramesh, S. Nadigar and S. Ramesh, *Antibiotics*, 2023, **12**, 532.

20 Mallappa, M. Chahar, N. Choudhary, K. K. Yadav, M. T. Qasim, R. Zairov, A. Patel, V. K. Yadav and M. Jangir, *J. Iran. Chem. Soc.*, 2025, **22**, 1–33.

21 R. J. Affrald and S. Narayan, *Russ. J. Bioorg. Chem.*, 2024, **50**, 824–854.

22 Y. Gao, F. Wang, C.-C. Wang and X.-H. Yi, *Surf. Interfaces*, 2024, **44**, 103724.

23 R. G. Faria, D. Julião, S. S. Balula and L. Cunha-Silva, *Compounds*, 2021, **1**, 3–14.

24 E. H. Lwanga, N. Beriot, F. Corradini, V. Silva, X. Yang, J. Baartman, M. Rezaei, L. van Schaik, M. Riksen and V. Geissen, *Chem. Biol. Technol. Agric.*, 2022, **9**, 20.

25 Z. Li, D. Liu, Y. Cai, Y. Wang and J. Teng, *Fuel*, 2019, **257**, 116031.

26 G. Calzaferri, S. H. Gallagher, S. Lustenberger, F. Walther and D. Brühwiler, *Mater. Chem. Phys.*, 2023, **296**, 127121.

27 D. Li, Y. Yang, D. Li, J. Pan, C. Chu and G. Liu, *Small*, 2021, **17**, 2101976.

28 A.-M. Brezoiu, L. Bajenaru, D. Berger, R.-A. Mitran, M. Deaconu, D. Lincu, A. Stoica Guzun, C. Matei, M. G. Moisescu and T. Negreanu-Pirjol, *Antioxidants*, 2020, **9**, 696.

29 A. Jabbar Khan, L. Gao, A. Numan, S. Khan, I. Hussain, M. Sajjad, S. S. Shah, A. Mateen and G. Zhao, *Crit. Rev. Solid State Mater. Sci.*, 2024, 1–24.

30 N. Parvin, S. W. Joo and T. K. Mandal, *Antibiotics*, 2025, **14**, 207.

31 D. Han, X. Liu and S. Wu, *Chem. Soc. Rev.*, 2022, **51**, 7138–7169.

32 L. Chen, Y. Liu, H. Zhang, Y. Li, S. Zhang, Y. Hu, H. Li and S. Yang, *React. Chem. Eng.*, 2023, **8**, 1464–1475.

33 N. Bouazizi, J. Vieillard, B. Samir and F. Le Derf, *Polymers*, 2022, **14**, 378.

34 Y. Etemadi, A. Shiri, H. Eshghi, M. Akbarzadeh, K. Saadat, S. Mozafari, H. Beyzaei and M. Moghaddam-Manesh, *J. Chem. Res.*, 2016, **40**, 600–603.

35 C. Mahapatra, R. Thakkar and R. Kumar, *Antioxidants*, 2024, **13**, 1172.

36 X. Chen, M. Li, M. Lin, C. Lu, A. Kumar, Y. Pan, J. Liu and Y. Peng, *J. Mater. Chem. B*, 2023, **11**, 5693–5714.

37 İ. Gulcin and S. H. Alwasel, *Processes*, 2023, **11**, 2248.

38 I. Kostova and L. Saso, *Curr. Med. Chem.*, 2013, **20**, 4609–4632.

39 B. Farasati Far, in *Logic for Metal–Organic Framework Selection: MOFs for Biomedical Applications*, ACS Publications, 2024, pp. 107–146.

40 M. Parcheta, R. Świsłocka, S. Orzechowska, M. Akimowicz, R. Choińska and W. Lewandowski, *Materials*, 2021, **14**, 1984.

41 J. Branković, N. Milivojević, V. Milovanović, D. Simijonović, Z. D. Petrović, Z. Marković, D. S. Šeklić, M. N. Živanović, M. D. Vukić and V. P. Petrović, *R. Soc. Open Sci.*, 2022, **9**, 211853.

42 A. Sharma, C. Soares, B. Sousa, M. Martins, V. Kumar, B. Shahzad, G. P. Sidhu, A. S. Bali, M. Asgher and R. Bhardwaj, *Physiol. Plant.*, 2020, **168**, 318–344.

43 A. Altharawi, S. M. Alqahtani, T. Aldakhil and I. Ahmad, *Front. Chem.*, 2024, **12**, 1386311.

44 A. H. Abdulkadhim, S. M. Husein Kamona, H. F. Shamikh Al-Saedi, A. G. Taki, A.-H. M. Hamoody, S. A. Hamood, S. O. Rab, A. A. Amir, A. T. Kareem and A. Alawadi, *Front. Chem.*, 2024, **11**, 1331933.

45 M. Moghaddam-manesh, G. Sargazi, M. Roohani, N. G. Zanjani, M. Khaleghi and S. Hosseinzadegan, *Polym. Bull.*, 2023, **80**, 11919–11930.

46 H. H. J. Al-Khafaji, A. Alsalamy, M. A. Jawad, H. A. Nasser, A. H. Dawood, S. Y. Hasan, I. Ahmad, M. A. Gatea and W. K. Y. Albahadly, *Front. Chem.*, 2023, **11**, 1236580.

47 Z. Ahani, M. Nikbin, M.-T. Maghsoodlou, F. Farhadi-Ghalati, J. Valizadeh, H. Beyzaei and M. Moghaddam-Manesh, *J. Iran. Chem. Soc.*, 2018, **15**, 2423–2430.

48 A. G. Alkhathami, W. Khaled Younis Albahadly, M. A. Jawad, M. F. Ramadan, K. M. Alsaraf, Z. A.-H. Riyad Muedii, F. Alsaikhan and M. Suliman, *Front. Mater.*, 2023, **10**, 1264529.

49 A. Altharawi, N. N. Jafar, T. Aldakhil and T. J. Kazem, *Inorg. Chem. Commun.*, 2024, **169**, 113092.

50 S. Sheikhi-Mohammareh, F. Oroojalian, H. Beyzaei, M. Moghaddam-Manesh, A. Salimi, F. Azizollahi and A. Shiri, *Talanta*, 2023, **262**, 124723.

51 H. Beyzaei, M. Kamali Deljoo, R. Aryan, B. Ghasemi, M. M. Zahedi and M. Moghaddam-Manesh, *Chem. Cent. J.*, 2018, **12**, 114.

52 T. M. Almeleebia, M. Jasim Naser, S. M. Saeed, M. M. Abid, U. S. Altimari, M. L. Shaghnab, F. A. Rasen, A. Alawadi, I. Ahmad and A. Alsalamy, *Front. Mater.*, 2024, **11**, 1354560.

53 S. A. Kozlovskiy, E. A. Pislyagin, E. S. Menchinskaya, E. A. Chingizova, Y. E. Sabutski, S. G. Polonik, G. N. Likhatskaya and D. L. Aminin, *Toxins*, 2023, **15**, 47.

54 H. Han, J.-K. Kang, K. J. Ahn and C.-G. Hyun, *BioChem*, 2023, **3**, 91–101.